Long distance offshore wakes

Bernardo Letsch[1], Leonardo Barriatto[1]

DNV Energy Systems

bernardo.letsch@dnv.com, leonardo.barriatto@dnv.com

ABSTRACT

The utilization of offshore wind energy has experienced significant growth since its conception in the 1970s, driven by advancements in turbine design, materials, and manufacturing techniques, enabling the development of larger and more powerful turbines and consequently increasing offshore wind farms' size and capacity. Nevertheless, a challenge faced by offshore wind farms is the aerodynamic interaction between wind turbines, wherein energy extraction from the wind creates regions of reduced wind speed and increased turbulence, impacting neighboring turbines' efficiency and productivity, leading to substantial energy losses. To tackle these challenges, numerical models have been developed to quantify and predict turbine interaction effects, considering factors such as atmospheric turbulence, wind speed, wind direction, and wake recovery. However, traditional single-fidelity models used in wind farm design oversimplify the physics and neglect critical physical influences, limiting their applicability to larger and more complex wind farms. Recent studies have highlighted the need for higher-fidelity modelling approaches, such as computational fluid dynamics (CFD) simulations coupled with mesoscale atmospheric modelling (WRF), which offer a more realistic representation of turbine interaction effects. These higher-fidelity models consider the coupled interactions between turbines and the atmosphere, and validation studies have demonstrated their accuracy in reproducing power production patterns observed in operational wind farms. By incorporating atmospheric stability and long-range wake propagation, these models provide improved predictions, particularly for larger and more complex wind farm configurations. As the offshore wind industry continues to expand, encompassing projects of unprecedented scales, it is crucial to adopt higher-fidelity turbine interaction models to ensure accurate assessments of energy production and to mitigate risks associated with larger projects. Embracing these advanced modelling approaches allows the offshore wind industry to optimize wind farm layouts, maximize energy production, and drive the transition towards a more sustainable and greener energy future.

Keywords:

Large offshore wind farms, aerodynamic interaction effects, numerical modelling, long cluster wakes.

1. INTRODUCTION: THE GROWTH OF OFFSHORE WIND FARMS

The utilization of offshore wind energy was first conceived in the 1970s. In 1991, the inaugural experimental offshore wind farm was established near the city of Vindeby [1], Denmark, consisting of 11 relatively small wind turbines with a capacity of 450 kW each. This marked the beginning of offshore wind power as a viable energy source.

Over the next two decades, more countries in Europe began investing in offshore wind farms, including the UK, Germany, the Netherlands, Belgium, and Sweden. These projects demonstrated the potential of offshore wind energy to generate large amounts of electricity and provided valuable experience for the industry.

The size of offshore wind farms has steadily grown over the years due to technological advancements in turbine design, materials, and manufacturing techniques that have enabled the development of larger, and more powerful turbines. The economies of scale have also played a role in this process. Larger turbines can generate more electricity, leading to a lower overall cost per unit of energy produced.

As the offshore wind industry grew, better infrastructure and specialized vessels were also developed to support the construction and maintenance of larger wind farms in more challenging marine environments. In addition to that, governments and energy companies around the world recognized the potential of offshore wind as a clean and renewable energy source, leading to increased investment and commitment to developing larger and more ambitious projects.

Some of the world's largest offshore wind farms have recently been built or are currently under construction. For example, the Hornsea One wind farm in the UK, which began operations in 2020, had a capacity of 1.2 gigawatts (GW). It is the largest operational offshore wind farm globally at present.

Figure 1-1 illustrates this trend for the operational offshore fixed-bottom wind turbines, which currently represent over 99.5% of the total power capacity of the global fleet (with floating wind turbines representing only 0.5% of that total).

Figure 1-1 : Worldwide average size of new fixed bottom offshore wind farms per year of start of operations

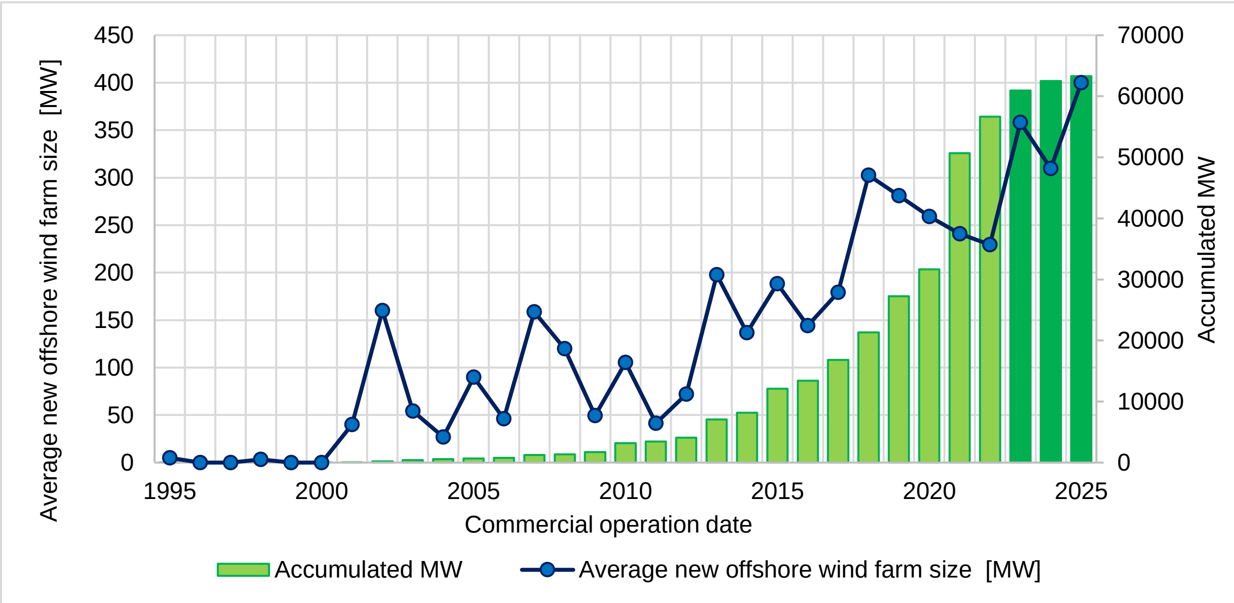

Source: DNV, December 2022.

The growth of modern wind turbines is not limited to their size and rated power; it also extends to the count of wind turbines per wind farm, which has been steadily increasing. As a result, modern wind farms are characterized by higher turbine densities, with turbines placed in relatively close proximity to each other. Consequently, turbine aerodynamic interactions emerge as a prominent challenge in the development of offshore wind farms, significantly impacting the efficiency and productivity of the turbines within the farm.

These aerodynamic interaction effects manifest as regions of reduced wind speed and increased turbulence surrounding each wind turbine as it extracts energy from the wind. With the escalation in both the number and size of turbines, the complexity of these interactions intensifies, as they mutually influence one another, thereby magnifying their adverse effects and leading to more pronounced energy losses. In light of these challenges, ongoing research and development efforts are directed toward developing and advancing numerical models that can accurately quantify and predict these phenomena.

2. DEVELOPMENT OF THE TURBINE INTERACTION MODELS

Turbine interaction models are the numerical methods used in the wind industry to quantify the interactions between operating wind turbines and the freestream atmospheric wind flow. These aerodynamic interaction effects are conventionally broken down into subcomponents: the wakes that develop downwind of the offshore wind farm, and the blockage or induction zone that develops upwind of the wind farm, considering the prevailing wind direction.

Figure 2-1 illustrates these interaction effects at a symbolic offshore wind farm composed of 105 wind turbines equally spread along an array of 7 rows. The hub-height from each turbine is 125 meters above sea level, and the rotor diameter is 174 meters. The physical conditions inside the surface boundary layer were set to resemble a neutral atmosphere.

Figure 2-1 : Top view of an offshore wind farm simulation with Computational Fluid Dynamics (CFD)

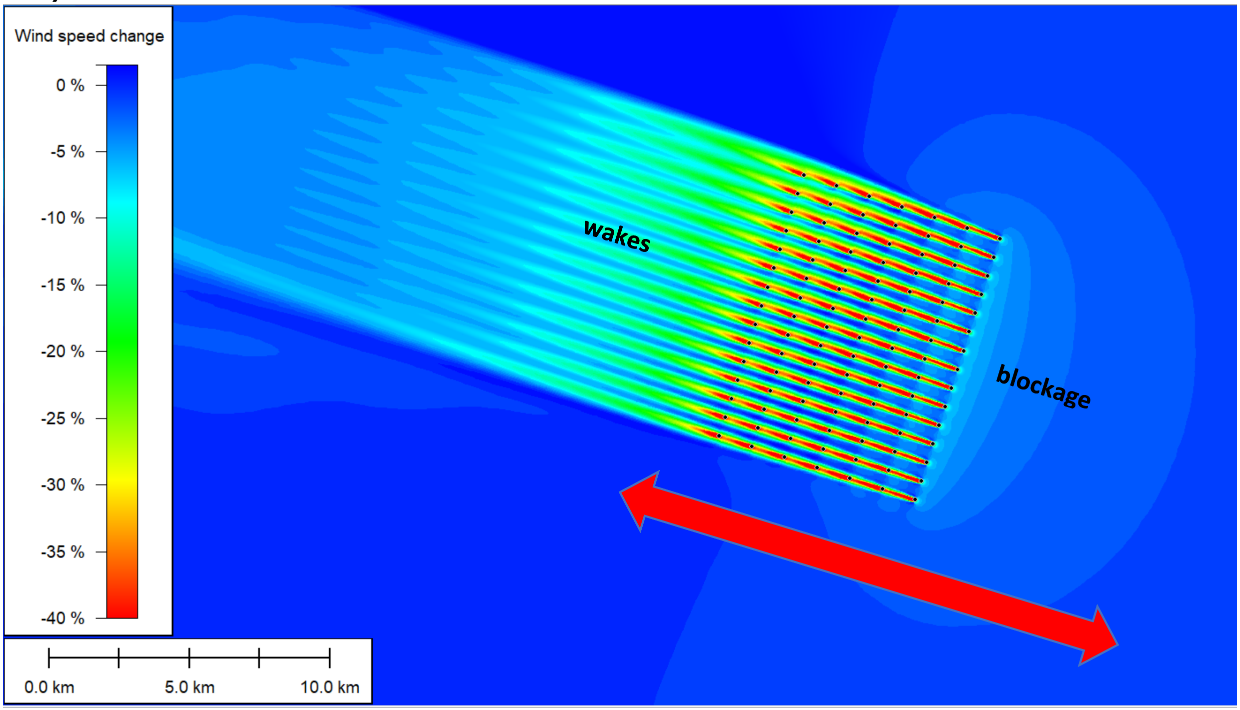

Source: DNV.

Most numerical models for turbine interaction effects consider factors like atmospheric turbulence, wind speed, wind direction, and wake recovery to quantify the impact of one operating turbine on its neighboring wind turbines. Understanding these interactions is essential for optimizing wind farm layouts, maximizing energy production, and ensuring efficient turbine operation. In offshore wind farms, the turbines are usually arranged in large arrays, where turbine interaction effects can have a significant impact on energy production.

Porté-Agel et al. [3] provided an extensive overview of the history of the numerical models for quantifying the wind turbine interaction effects. The authors also summarized the latest experimental, computational, and theoretical research endeavours that have played a crucial role in enhancing human comprehension and predictive capabilities concerning the interactions between the atmospheric boundary layer (ABL) flow and wind farms.

The models for wind turbines' interactions have been evolving since the early 1980s. Researchers and wind energy developers continue to improve and refine these models to enhance their accuracy and applicability in real-world scenarios. But regardless of their specific nature or age, most numerical models tend to follow a similar cost-fidelity relationship. Typically, the more advanced the physics or fidelity of the numerical model, the more expensive it is to execute or solve. Figure 2-2 provides a qualitative illustration of DNV's view of this cost-fidelity trend that is inherent to the turbine interaction models.

Figure 2-2 : Cost-fidelity relationship for an arbitrary selection of turbine interaction models

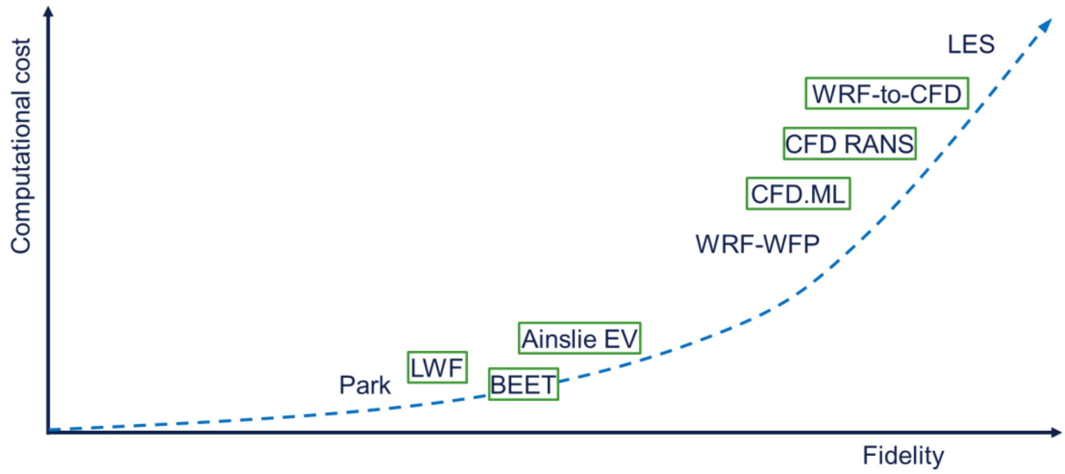

Source: DNV.

The list of existing models is extensive, and Figure 2-2 presents only a particular collection of models that are known by DNV to be frequently used in the wind industry and academy. The models encapsulated by green boxes are the ones currently applied by DNV during the development phase of offshore commercial wind farms across the globe.

This collection includes the Park wakes-only model, proposed by Jensen in 1983 [4][5]. The Large Wind Farm (LWF) correction model [6][7]. The Blockage Effect Estimator Tool (BEET) [14], and the Eddy Viscosity (EV) wakes-only model based on work conducted by Ainslie [9][10].

The models populating the lower left corner of Figure 2-2 are commonly labelled "engineering models". This terminology typically refers to a simplified representation of a complex system or process that is used by engineers to analyse, understand, and predict its behaviour. For the purpose of this paper, the term "single-fidelity" models will be used to describe these models due to their simplified approach to physics. These models often decompose the intricate aerodynamic interactions imposed by a wind farm on the free atmosphere into theoretical and simplified components. Consequently, they exclusively address or simulate individual components separately.

Among these models, some are referred to as ''wakes-only'' models, as they exclusively solve for the average flow downstream of the rotors in the far-wake region. Others fall under the category of ''induction-only'' models, which focus solely on the phenomena occurring upwind of the turbines within the induction or blockage zone. Additionally, there exists a type of model known as the large wind farm (deep array) model, which emphasizes the two-way coupling between wind farms and the atmospheric wind flow. Traditional software utilized for wind energy production forecasts then aggregates the outcomes of each single-fidelity model, considering them as distinct physical phenomena in isolation.

It is essential to emphasize that single-fidelity models are characterized by their cost-effectiveness and fast execution. Due to these advantages, they still play a crucial role in wind farm design, particularly in layout optimization. Furthermore, many of the models presented in the lower-left corner of Figure 2-2 have been well validated against real data collected from different operational offshore wind farms in the past. Notable examples of validation cases commonly employed for single-fidelity interaction models include (but are not limited to) the Vindeby wind farm, which was operational off the coast of Denmark from 1991 to 2017, boasting a rated capacity of 4.95 MW [11]. Similarly, the Horns Rev I wind farm, operating in the North Sea since 2002 with a total capacity of 160 MW, and the Nysted (Rødsand I) wind farm, operational in the Baltic Sea since 2003 with 166 MW capacity, have been widely utilized for validation purposes [12].

In numerous instances, single-fidelity models for turbine interaction have also been fine-tuned and calibrated using operational data from early offshore wind farms. However, as discussed in section 0, the offshore wind farms of the future are expected to be larger and more complex in many cases. Due to the simplified approach to physics inherent in these single-fidelity models, they tend to overlook critical physical influences. As a result, they cannot be expected to generalize beyond the conditions of their validation envelope.

3. EXTRAPOLATING THE VALIDATION ENVELOPE

Repeated experiments conducted using real data from more contemporary and larger wind farms have begun to reveal indications that many of the technical assumptions underlying the validation and fine-tuning of single-fidelity models in the past are gradually becoming obsolete.

For example, the Large Wind Farm (LWF) correction model [8] has extensively been deployed with a maximum downstream recovery distance set to 60 rotor diameters, under the assumption that after this distance downwind of a wind farm, the wind speed would fully recover to the ambient (freestream) levels. Similarly, widely employed software in the offshore wind industry defaulted to a maximum wake length of 50 rotor diameters for the Eddy Viscosity (EV) wakes-only model [15]. However, recent field experiments using empirical data have demonstrated that these distances are inadequate when compared to observed wakes in modern operational wind farms.

In a study led by Williams [13], DNV investigated the relative power generation recorded by two modern wind turbines belonging to the same offshore wind farm in the North Sea. This investigation was conducted for wind directions in which only one of these wind farms would be affected by the wakes generated from a neighboring operational wind farm, located approximately 200 rotor diameters upstream. The relative layout of these wind farms is presented in Figure 3-1.

Figure 3-1 : Relative position of the wind farms being assessed in the North Sea

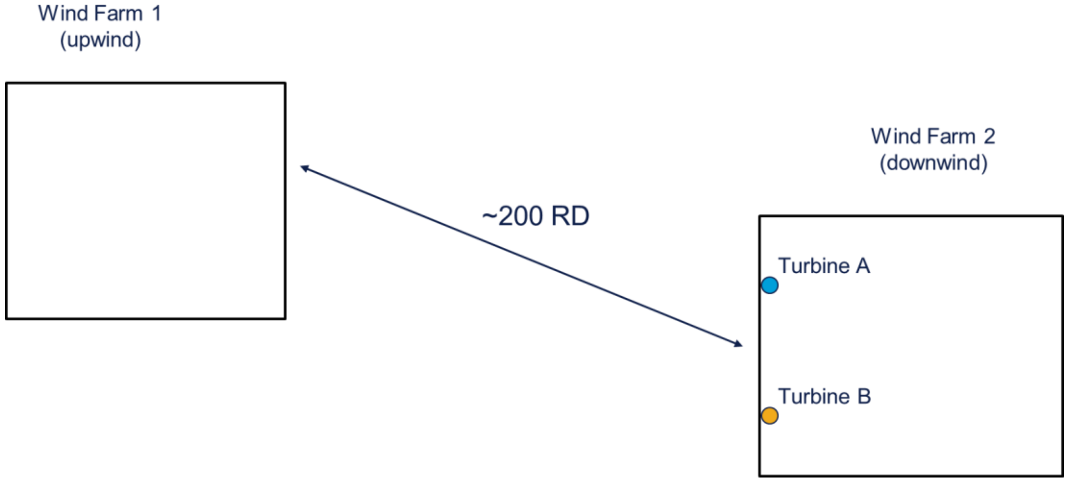

Source: DNV [13].

Approximately 3 years of operational data (SCADA) from each of the wind farms were analysed. The hub heights of the rotors ranged from 80 m to 120 m above sea level, and the rotor diameters varied between 100 m and 150 m.

When the wind blows from the direction of 270° (relative to true north), turbine ''A'' in the first row of wind farm 2 is affected by the wake generated by wind farm 1 operating upstream. The data collected by the SCADA system from these turbines and analysed by DNV demonstrate that under these conditions, turbine ''A'' generates approximately 15% less power than turbine ''B'', which would be free from external wakes. This situation is illustrated in Figure 3-2.

Figure 3-2 : Power ratio between front row turbines 'A' and 'B'. Wind direction from 270° degrees.

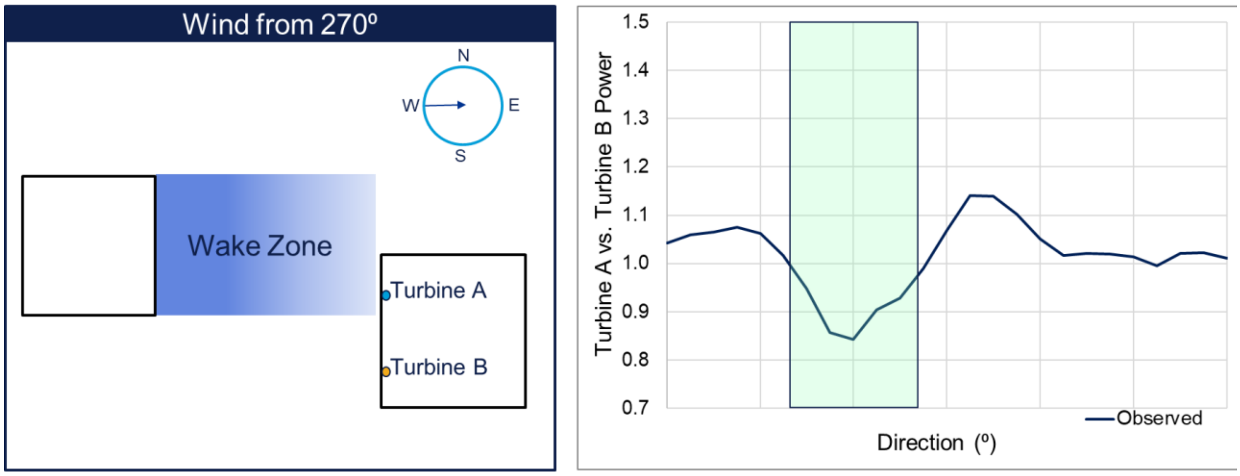

Source: DNV [13].

When the wind flow originates from the direction of 310° (relative to true north), turbine 'B' in the first row of wind farm 2 is affected by the wake generated by wind farm 1 operating upstream. The analysed data suggests that under these conditions, turbine 'B' generates approximately 15% less power than turbine 'A'. This situation is illustrated in Figure 3-3.

For the remaining wind flow directions, the power generation ratio between turbines 'A' and 'B' is closer to 1.0 when both are free from the external wake effects generated by wind farm 1, considering the 3 years of analysed data.

Figure 3-3 : Power ratio between front row turbines 'A' and 'B''. Wind direction from 310° degrees.

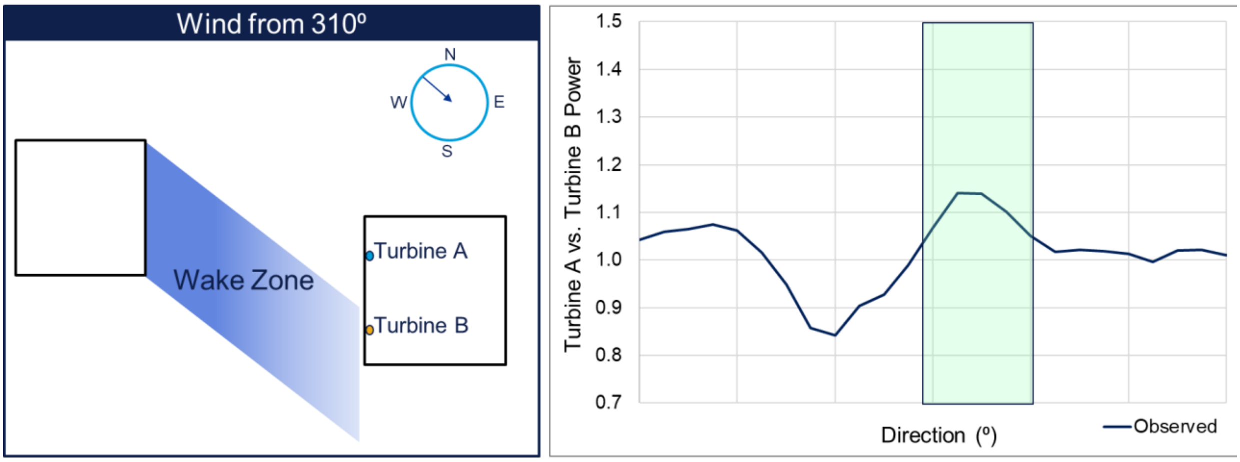

Source: DNV [13].

So, according to these findings, the wake formed by the operation of a large wind farm was intense enough to cause a power deficit of 15% in neighboring wind turbines even after travelling over 200 rotor diameters (~ 20 km) through the North Sea. Many single-fidelity wakes-only models would predict this power deficit to be negligible at this distance.

In a second study, Schneemann et al. [16] evaluated the Global Tech I (GTI) offshore wind farm, with 400 MW of installed capacity, located in German waters in the North Sea. This wind farm is accompanied by four other operational neighboring wind farms, situated at distances of up to 55 km, as illustrated in Figure 3-4.

A long-range horizontal scanning LiDAR remote sensor (model WindCube 200S) was mounted on a fixed platform located within the wind farm's perimeter, and its measurements were compared with Synthetic Aperture Radar (SAR) measurements from the European space agency's Sentinel-1A monitoring satellite.

Figure 3-4 : a) Horizontal mean wind speed field, as measured by SAR satellite. Wind blowing from the southeast sector. B) GTI wind farm location, in relation to neighbour wind farms.

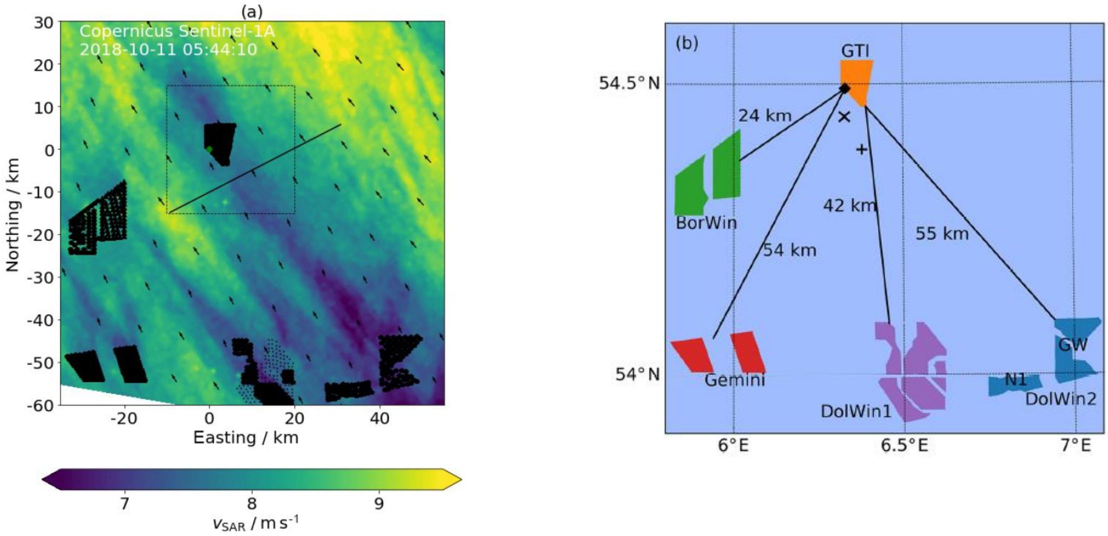

Source: Schneemann et al. [16] (Creative Commons license).

Upon analyzing the measured data, the authors concluded that during conditions of stable atmospheric stability [1](typically when hot air masses flow over cold waters), wakes have travelled 55km, originating from the DolWin2 wind cluster and reaching the GTI wind farm. These super-long cluster wakes persisted for periods of 2.5 hours and caused wind speed reductions of up to 21% (-2.2 m/s) in the first rows of the GTI park.

In a third study, Platis et al.[17] used a specially instrumented aircraft to directly measure the wakes produced by large offshore wind farms in the North Sea, operating near the border between Germany and Denmark. A total of 41 flights were performed, at a constant altitude of 90 m above sea level, on a pre-defined route downwind of the wind farms, presented in Figure 3-5. The altitude chosen is representative of the hub height of the wind farms located in the vicinity of the flight path.

Figure 3-5 : Flight track. The locations of Amrumbank West, Nordsee Ost e Meerwind Süd/Ost wind farms, as well as the FINO1 station are also shown.

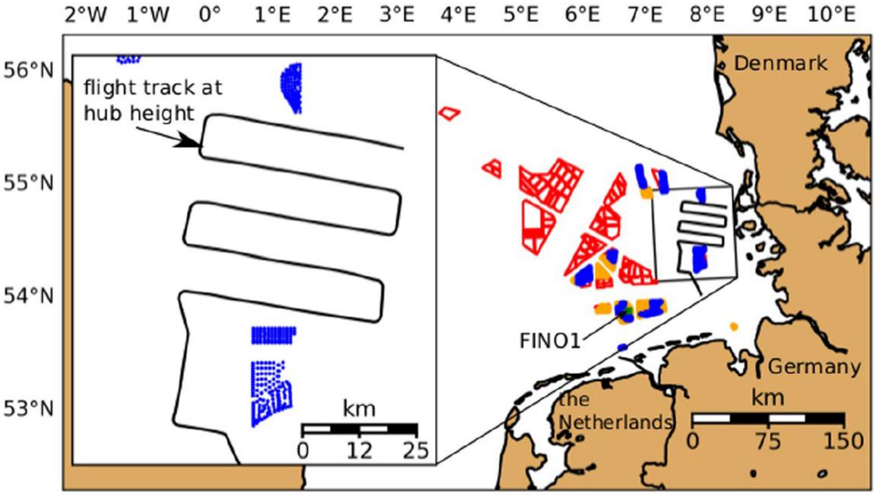

Source: Platis et al. [17] (Creative Commons license).

Each overflight lasted between 3 and 4 hours, depending on the daily weather conditions. Throughout the 6-month data collection period, the authors were able to cover different atmospheric conditions: stability, neutrality, and instability. Using instruments installed on the aircraft specifically for this purpose, it was possible to reconstruct the horizontal component of wind velocity in the region upstream of the following offshore wind farms: Amrumbank West, Nordsee Ost, and Meerwind Süd/Ost.

Based on the data they collected, the authors found evidence of offshore wakes propagating up to:

- 55 km when the atmospheric boundary layer was stable (warm air mass over cold water).
- 35 km when the atmospheric boundary layer was in a neutral condition.
- 10 km when the atmospheric boundary layer was unstable (cold air mass over warm water).

The aerodynamic interactions investigated in the independent studies conducted by Williams [13], Schneemann et al. [16] and Platis et al.[17] exhibit substantial magnitudes. These interactions are significantly more intense and propagate over considerably greater distances compared to the samples

[1] Atmospheric stability is a measure of the atmospheric condition that determines whether air masses will rise, descend, or remain neutral. In general, an unstable atmosphere will enhance or promote vertical air movement, a stable atmosphere will suppress or resist vertical movement, and a neutral atmosphere will neither suppress nor enhance vertical movement.

utilized for validating and refining the wakes-only single-fidelity models developed in the early 1980s [11][12].

The single-fidelity models incorporate physics and mathematical simplifications, rendering them fast and efficient. Consequently, they have become indispensable in wind farm design and analysis. However, the issue lies in the exclusive reliance on these models when more reliable and higher-fidelity alternatives are available. Wind projects valued at over a billion euros are routinely financed and constructed without undergoing assessments employing anything beyond a basic wakes-only model and a separate, even simpler, blockage model.

4. HIGHER-FIDELITY MODELLING AND FURTHER VALIDATIONS

In the context of this work, the higher-fidelity models are those capable of reproducing the aerodynamic interactions between the operating wind turbines and the atmosphere with greater physical realism. The physical phenomena at play are no longer assessed as independent components but are rather solved for their coupled interactions.

CFD RANS, or the deployment of the Reynolds-Averaged Navier-Stokes (RANS) equations within a Computational Fluid Dynamics (CFD) domain is perhaps of one the most cost-effective solutions within these higher-fidelity models.

DNV's CFD service to model flow conditions within and around wind farms solves the steady-state RANS equations, using the k-ε model for turbulence closure, with a modified set of constants [21]. DNV customized the model for simulating the atmosphere at wind-farm-scale, with emphasis on accounting for thermal stratification both within and above the boundary layer (BL) [21], [22] .This is done by accounting for buoyancy effects in the vertical momentum equation and in the turbulence model, using a shallow Boussinesq formulation [22]. The effect of the Coriolis force and the associated development of an Ekman spiral are also modelled, implementing the Coriolis force in the horizontal momentum equations.

In these CFD simulations, the turbine interaction losses are captured by modelling the turbines with actuator disks [26]. The disk volumes comprise cubic mesh cells with edge lengths equal to 5% of the rotor diameter (20 cells across the rotor diameter and 5 cells across the disk thickness). The axial and tangential body forces applied to the cells ultimately derive from manufacturer-provided curves for power and thrust coefficient. Through these simulations it is possible to quantify for each individual turbine the difference between its power production in isolation and its production when the other wind farm turbines are present. This wind farm model has been validated across a range of commercial projects, with a limited set of validation results presented in [27] and [28].

To better represent the offshore inflow conditions that are imposed to the boundaries of the CFD numerical domain and enable the accurate simulation of the mesoscale thermal effects within and above the atmospheric boundary layer, DNV has recently been investigating the coupling between Weather Research and Forecast (WRF) modelling and its CFD RANS engine.

WRF [23] is a mesoscale transient numerical weather prediction system that is suitable for running high-resolution simulations with horizontal grid spacing down to 1-2 km. WRF is developed and maintained by a consortium of more than 150 international agencies, laboratories, and universities. Data is typically produced as virtual hourly time series on a high-resolution grid, centred on the site or wind farm under consideration. The outputs of the WRF simulations are then time-averaged and used to derive the inflow boundary conditions for CFD simulations.

These simulations for turbine interaction effects naturally account for long cluster wakes superposition effects, by enforcing mass, momentum and energy conservation. Contrary to the single-fidelity models, they do not require ad hoc assumptions about these superpositions.

This new WRF-to-CFD model developed was used by Montavon et al.[28] to quantify the turbine interaction effects on two offshore operational neighboring wind farms in the North Sea, namely Hohe See and Albatros, which combined sum to over 639 MW of power capacity. The WRF simulation was run with 4 nested domains, with resolutions starting from 62 km x 62 km and reaching a final grid with a horizontal resolution of 1 km. The model included simulations for 41 atmospheric levels, up to a 19.3km altitude, and its initial conditions were driven by the ERA-5 reanalysis [24], during a period concurrent with the measurement campaign (Nov 2021 – Feb 2023). The simulations were performed multiple times, to generate various sets of both stable and unstable atmospheric boundary conditions for the CFD RANS engine.

These offshore wind farms along with their operational neighbours, and a heat map of interaction effects calculated with WRF-to-CFD at 105 meters above sea level are presented in Figure 4-1.

Figure 4-1 : Neighbour wind farms operating approximately 18km upwind of Hohe See and Albatros. WRF-to-CFD simulations for Wind direction: 268°. Unstable atmospheric conditions.

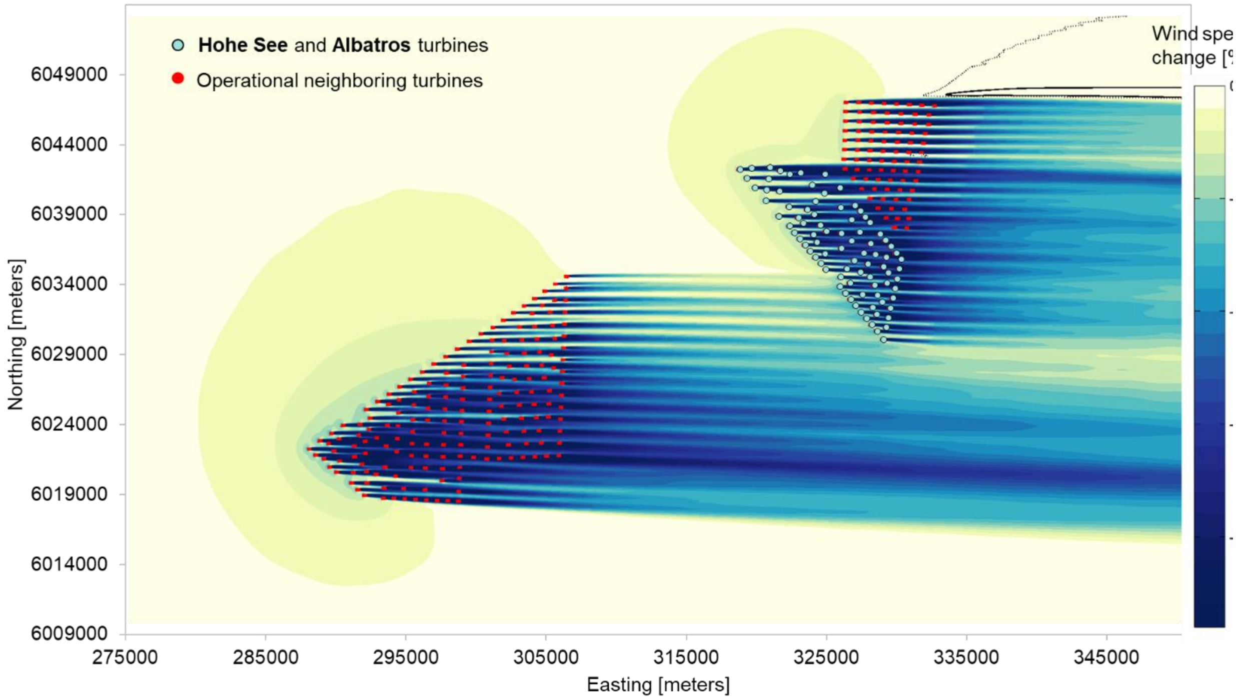

Source. DNV [28].

CFD-based predictions were utilized to estimate the energy production of wind turbines, and the results were compared with the actual power production data recorded by the Supervisory Control and Data Acquisition (SCADA) systems. This comparison facilitated the validation of the CFD-predicted distribution of energy production within the wind farms. To ensure accuracy, the historical operational data underwent appropriate filtering based on wind turbine availability (>85%), wind direction, and atmospheric conditions.

One of the many such comparisons investigated by Montavon et al.[28] is presented in Figure 4-2, for a period when the wind farm was operating under unstable atmospheric conditions and the wind was blowing from the west.

Figure 4-2 : Normalized power: measured and simulated. Unstable atmospheric conditions. Wind direction: 268°.

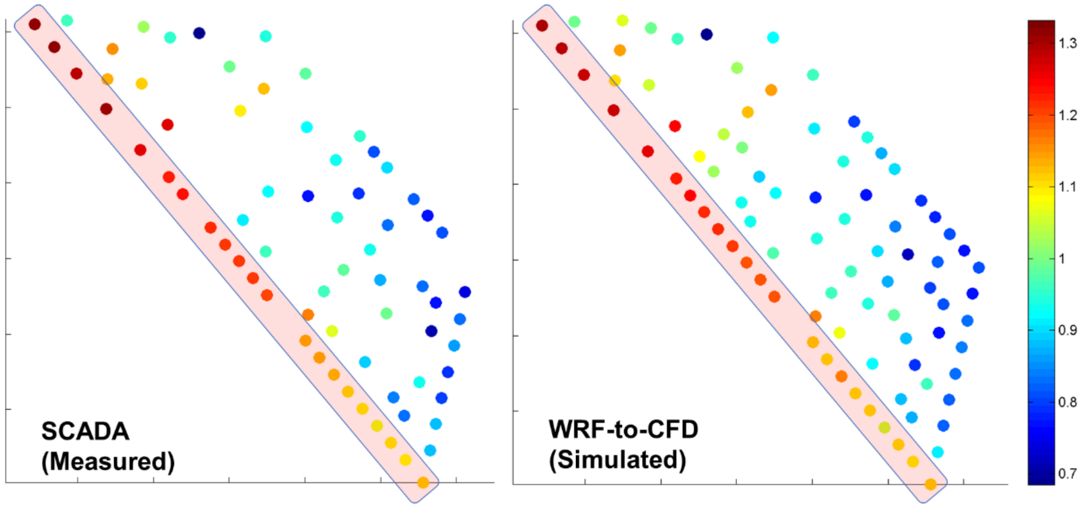

Source. DNV [28].

A similar comparison, made only with the front-row turbines of Hohe See and Albatros, is presented in Figure 4-3. The numerical simulations with WRF-to-CFD were able to capture very well the distribution of power within the Albatros and Hohe See projects, including the first row's pattern of production. It's also worth noting that there's a large variation of power across the line of leading turbines, with the lowest producing 20% less than the highest producing turbine. This difference is primarily due to the recovering cluster wakes from the upstream neighbouring wind farms sited over 18 km away.

Figure 4-3 : Normalized power for front row turbines: measured and simulated. Unstable atmosphere. WD: 268°.

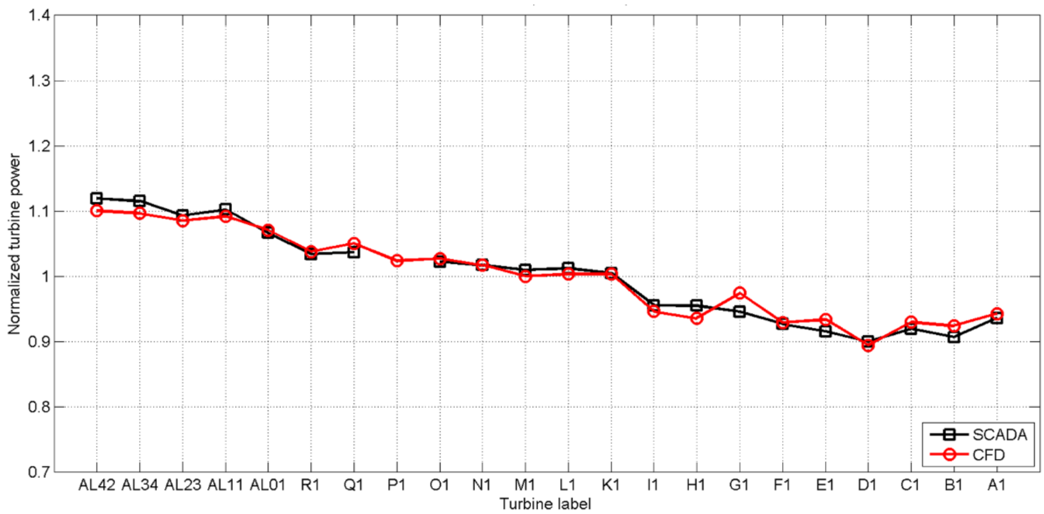

Source. DNV [28].

The same exercise was repeated, but instead of filtering the operational data for moments when the surface boundary layer was presenting stable behaviour. Likewise, the equivalent set of numerical WRF-to-CFD simulations was re-run with the proper modifications to represent these same conditions. The heat map of horizontal wind speed deficit for one of these simulations is presented in Figure 4-3.

Figure 4-4 : Neighbour wind farms operating at approximately 18km upwind of Hohe See and Albatros. WRF-to-CFD simulations for wind direction 268°. Stable atmospheric conditions.

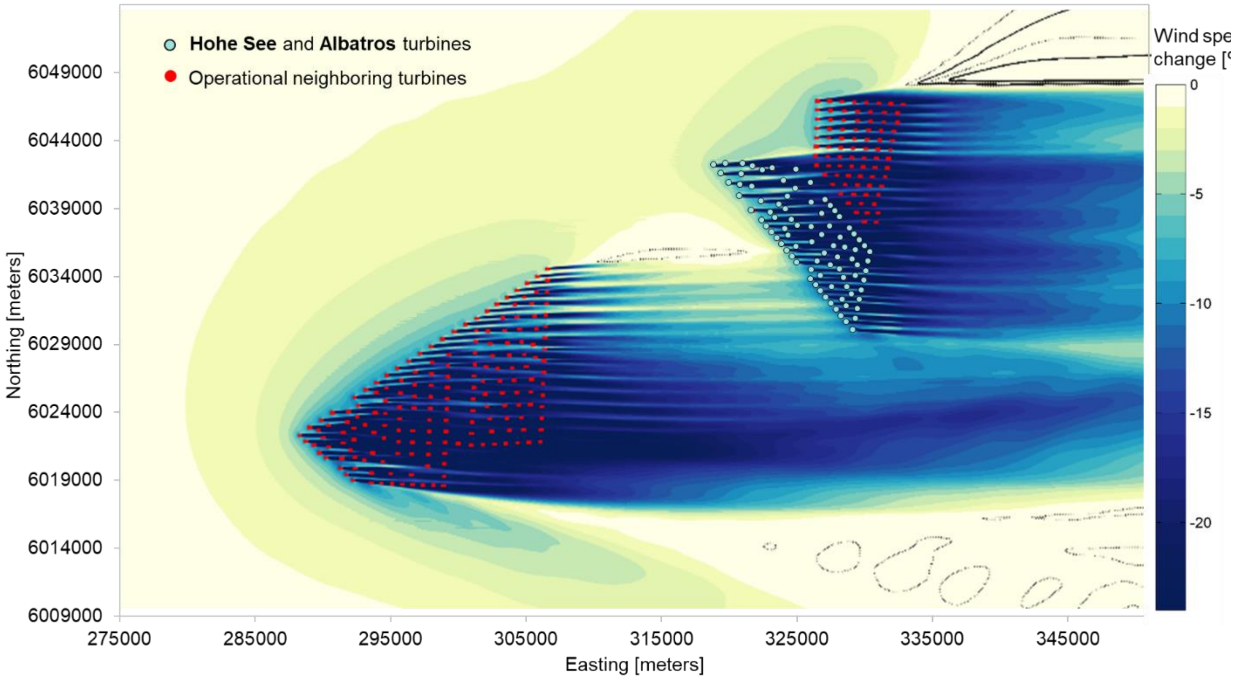

Source. DNV [28].

Figure 4-5 illustrates the normalized power production of the primary turbines in the Albatros and Hohe See projects. These results are derived from a new series of numerical simulations conducted under stable atmospheric conditions and are compared with the power production data obtained from filtered operational SCADA records. Once again, the utilization of WRF-to-CFD numerical simulations yielded excellent accuracy in capturing the power distribution patterns within the Albatros and Hohe See projects, including the production pattern observed in the first row of turbines. Notably, the discrepancy in power output among the leading turbines has significantly increased, with the lowest-performing turbine producing 33% less power than the highest-performing turbine. That's a clear register of large offshore cluster wakes travelling over 18 km and still being able to considerably lower the performance of a downwind wind farm.

Figure 4-5 : Normalized power for front row turbines: measured and simulated. Stable atmosphere. WD: 268°.

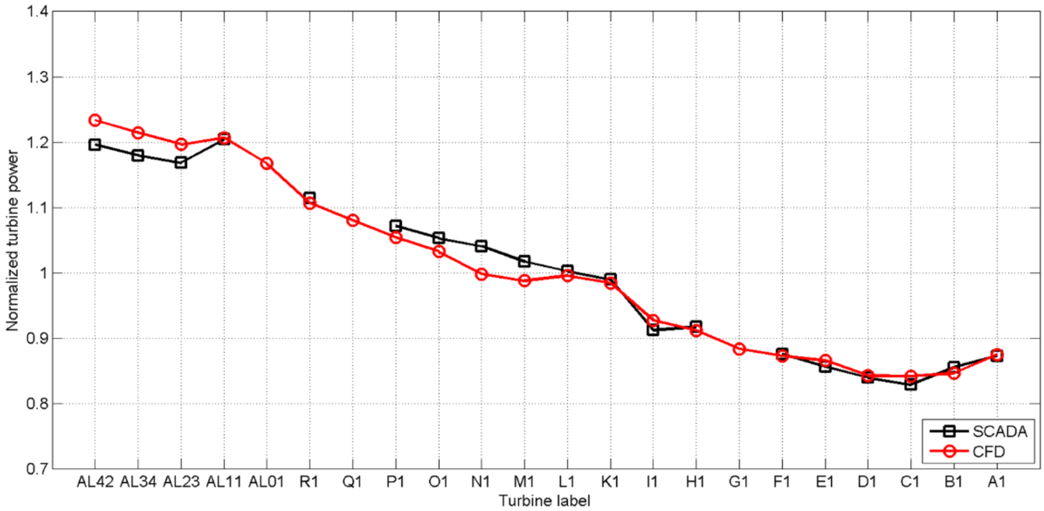

Source. DNV [28].

5. DISCUSSION AND CONCLUSION

In conclusion, the findings of this study demonstrate that the increase in wind farm capacity density, larger turbines, and regional clustering will lead to the extended propagation distances of offshore cluster wakes. Empirical evidence and measurements have shown that under stable atmospheric conditions, the wakes formed downwind and the blockage zone formed upwind of offshore wind farms can propagate over considerably longer distances and may be up to twice as intense compared to neutral or unstable atmospheric conditions.

The measurements and numerical simulations conducted by DNV using the latest WRF-to-CFD model for turbine aerodynamic interactions have further supported these findings. It is important to note that many of the single-fidelity models currently utilized in the wind industry do not explicitly consider atmospheric stability. Therefore, incorporating atmospheric stability into models will result in a more accurate representation of wakes over long distances.

While single-fidelity models are suitable for early design phases and optimization exercises due to their cost-effectiveness, it should be acknowledged that Brazilian offshore wind projects are expected to be significantly large, surpassing the validation envelopes of these models. To mitigate the risks associated with these larger projects, DNV strongly recommends the utilization of high-fidelity turbine interaction models capable of accurately simulating both internal and external turbine interaction effects.

An analysis performed with a higher-fidelity model enhances accuracy and provides detailed insights into turbine interaction effects within the wind farm, surpassing the capabilities of single-fidelity models. WRF-to-CFD simulations, due to their improved representation of the physics surrounding wind farms, are significantly more capable than single-fidelity models in delivering scalable results as turbine and wind farm sizes increase. This mitigates the risk of systematic biases in numerical predictions when applied to future wind farms that greatly differ in size from those in the current validation datasets.

ACKNOWLEDGMENTS

The authors would like to express sincere gratitude to Christiane Montavon and James Bleeg for their immense contributions in advancing and validating the numerical modelling of aerodynamic interaction effects in large offshore wind farms. Their combined work and research have broken new ground and have been of paramount importance to the wind industry worldwide in recent years. Additionally, the authors would like to thank EnBW and Enbridge for granting permission to make the validations conducted at the Hohe See and Albatros offshore wind farms public.

6. BIBLIOGRAPHIC REFERENCES

[1] "Making Green Energy Affordable How the Offshore Wind Energy Industry Matured – and What We Can Learn from It." *1991-2001 The First Offshore Wind Farms (Chapter 2/6)* | Ørsted, orsted.com/en/insights/white-papers/making-green-energy-affordable/1991-to-2001-the-first-offshore-wind-farms. Accessed 1 July 2023.

[2] "Hornsea 1 Offshore Wind Farm." *Hornsea One - Offshore Wind Farm* | Ørsted, orsted.co.uk/energy-solutions/offshore-wind/our-wind-farms/hornsea1. Accessed 1 July 2023.

[3] Porté-Agel, Fernando, et al. "Wind-Turbine and Wind-Farm Flows: A Review." *Boundary-Layer Meteorology*, vol. 174, no. 1, 2019, pp. 1–59, https://doi.org/10.1007/s10546-019-00473-0.

[4] N, Jensen, "A note on wind generator interaction," RISØ M-2411, 1983.

[5] Katic I, Høstrup J and Jensen N, "A simple model for cluster efficiency," in EWEC, 1986.

[6] Schlez, W., Neubert, A and Smith, G M, "New Developments in Precision Wake Modelling," in DEWEK, Bremen, 2006.

[7] Schlez, W. Neubert, A., "New Developments in Large Wind Farm Modelling," in EWEC, Marseille, France, 2009.

[8] Large Wind Farm Correction | Windfarmer Documentation, dnvgldocs.azureedge.net/WindFarmer:%20Analyst_Latest/CalcRef/TurbineInteractions/LargeWindFarmCorrection/largeWindFarmCorrection.html. Accessed 5 July 2023.

[9] F, Ainslie J, "Development of an eddy viscosity model for wind turbine wakes," in Proceedings of 7th BWEA Wind Energy Conference, Oxford, 1985.

[10] F, Ainslie J, "Development of an Eddy Viscosity model of a Wind Turbine Wake," CERL Memorandum TPRD/L/AP/0081/M83, 1983.

[11] "Windfarmer Validation Report, Version 5.3". Garrad Haasan & Partners Ltd. April 2014.

[12] "Windfarmer White Paper, April 2016. DNV." www.dnv.com/publications/windfarmer-white-paper-april-2016-65253. Accessed 2 July 2023.

[13] Williams, Ben. "Far-distant offshore wakes: How far is too far and are we getting it right*?". Wind Europe Technology Workshop 2022.* https://windeurope.org/tech2022/proceedings/.

[14] "Wind Farm Blockage." WindFarmer Documentation, dnvgldocs.azureedge.net/WindFarmer:%20Analyst_Latest/CalcRef/TurbineInteractions/BlockageModel/blockageModel.html. Accessed 4 July 2023.

[15] LLC, UL Renewables. "Openwind Online Help." Basic Wake Models, openwind.ul-renewables.com/basicwakemodels.html. Accessed 4 July 2023.

[16] Schneemann, Jörge, et al. "Cluster Wakes Impact on a Far-Distant *Offshore* Wind Farm's Power." *Wind Energy Science*, vol. 5, no. 1, 3 Jan. 2020, pp. 29–49., https://doi.org/10.5194/wes-5-29-20.

[17] Platis, Andreas, et al. "First in Situ Evidence of Wakes in the Far Field behind *Offshore* Wind Farms." *Scientific Reports*, vol. 8, no. 1, 1 Fev. 2018, https://doi.org/10.1038/s41598-018-20389-y.

[18] Fitch A.C, Olson J.B, Lundquist J.K., Dudhia J, Gupta A.K., Michalakes J., Barstad I. Local and mesoscale impacts of wind farms as parameterized in a mesoscale NWP model. Monthly Weather Review. 2012; 140: 3017– 3038.

[19] Fitch, A. C. (2016) Notes on using the mesoscale wind farm parameterization of Fitch et al. (2012) in WRF. Wind Energ., 19: 1757– 1758. doi: 10.1002/we.1945.

[20] T Levick *et al* 2022 J. Phys.: Conf. Ser. 2257 012010.

[21] Bleeg, J.; Digraskar, D.; Woodcock, J.; Corbett, J. F. Modeling Stable Thermal Stratification and Its Impact on Wind Flow over Topography. Wind Energy, Wiley Online, 14 Jan. 2014, https://onlinelibrary.wiley.com/doi/10.1002/we.1692/.

[22] Bleeg, J.; Digraskar, D.; Horn. U.; Corbett, J. F. Modelling stability at microscale, both within and above the atmospheric boundary layer, substantially improves wind speed predictions. Proceedings from EWEA, Paris, France, 2015.

[23] Weather Research and Forecasting Model, https://www.mmm.ucar.edu/weather-research-and-forecasting-model.

[24] The European Centre for Medium-Range Weather Forecasts (ECMWF); ERA-5; website at https://www.ecmwf.int/en/forecasts/datasets/archive-datasets/reanalysis-datasets/era5.

[25] Montavon, Christiane, et al. Blockage and cluster-to-cluster interactions from dual scanning lidar measurements. Wind Energy Science (WESC) 2023, Glasgow. https://doi.org/10.5281/zenodo.8000511.

[26] Van der Laan, M.; Sørensen, N.N.; Réthoré, P.E.; Mann, J.; Kelly, M.C. "The k-ε-fp model applied to double wind turbine wakes using different actuator disk force methods". Wind Energy 2014, doi:10.1002/we.1816.

[27] Bleeg, J.; Purcell, M.; Ruisi, R.; Traiger, E. "Wind Farm Blockage and the Consequences of Neglecting Its Impact on Energy Production". Energies 2018, 11, 1609. Available at http://www.mdpi.com/1996-1073/11/6/1609.

[28] C. Montavon, J. Bleeg, J. Riechert, M. Steger, S. Soderberg, C. Schmitt, 'Measuring and Modelling Wind Farm Blockage Offshore', Wind Europe WRA Technical Workshop 2021, https://windeurope.org/tech2021/proceedings/.